

Clathrin Mediates Infectious Hepatitis C Virus Particle Egress

Ignacio Benedicto,^{a,b*} Virginia Gondar,^{a,b} Francisca Molina-Jiménez,^a Luisa García-Buey,^{b,c} Manuel López-Cabrera,^d Pablo Gastaminza,^e Pedro L. Majano^{a,b}

Molecular Biology Unit, Hospital Universitario de la Princesa, Instituto de Investigación Sanitaria Princesa (IP), Madrid, Spain^a; CIBERehd, Instituto de Salud Carlos III, Madrid, Spain^b; Liver Unit, Hospital Universitario de la Princesa, Instituto de Investigación Sanitaria Princesa (IP), Madrid, Spain^c; Centro de Biología Molecular Severo Ochoa, CSIC-UAM, Madrid, Spain^d; Centro Nacional de Biotecnología-CSIC, Madrid, Spain^e

ABSTRACT

Although it is well established that hepatitis C virus (HCV) entry into hepatocytes depends on clathrin-mediated endocytosis, the possible roles of clathrin in other steps of the viral cycle remain unexplored. Thus, we studied whether cell culture-derived HCV (HCVcc) exocytosis was altered after clathrin interference. Knockdown of clathrin or the clathrin adaptor AP-1 in HCVcc-infected human hepatoma cell cultures impaired viral secretion without altering intracellular HCVcc levels or apolipoprotein B (apoB) and apoE exocytosis. Similar reductions in HCVcc secretion were observed after treatment with specific clathrin and dynamin inhibitors. Furthermore, detergent-free immunoprecipitation assays, neutralization experiments, and immunofluorescence analyses suggested that whereas apoE associated with infectious intracellular HCV precursors in endoplasmic reticulum (ER)-related structures, AP-1 participated in HCVcc egress in a post-ER compartment. Finally, we observed that clathrin and AP-1 knockdown altered the endosomal distribution of HCV core, reducing and increasing its colocalization with early endosome and lysosome markers, respectively. Our data support a model in which nascent HCV particles associate with apoE in the ER and exit cells following a clathrin-dependent transendosomal secretory route.

IMPORTANCE

HCV entry into hepatocytes depends on clathrin-mediated endocytosis. Here we demonstrate for the first time that clathrin also participates in HCV exit from infected cells. Our data uncover important features of HCV egress, which may lead to the development of new therapeutic interventions. Interestingly, we show that secretion of the very-low-density lipoprotein (VLDL) components apoB and apoE is not impaired after clathrin interference. This is a significant finding, since, to date, it has been proposed that HCV and VLDL follow similar exocytic routes. Given that lipid metabolism recently emerged as a potential target for therapies against HCV infection, our data may help in the design of new strategies to interfere specifically with HCV exocytosis without perturbing cellular lipid homeostasis, with the aim of achieving more efficient, selective, and safe antivirals.

Several cellular factors have been described as mediators of hepatitis C virus (HCV) assembly, including components of the very-low-density lipoprotein (VLDL) synthesis machinery (1). Indeed, nascent virions are thought to exit the infected hepatocyte by traveling along the secretory pathway tightly linked to VLDL exocytosis. This is based on the observation that around 40% of HCV RNA in plasma samples from infected patients is found in a low-density fraction in association with triglyceride-rich lipoproteins containing apolipoprotein B (apoB) and apoE (2). Concordantly, it is well established that apoE is essential for cell culture-derived HCV (HCVcc) assembly and egress (3). Furthermore, apoE has been shown to interact with HCVcc, being an important determinant of HCVcc infectivity (4). In addition, it has been suggested that microsomal triglyceride transfer protein (MTP) and apoB also participate in HCVcc morphogenesis and secretion (5), although these data remain controversial (6). In sum, although it is widely accepted that HCV and VLDL morphogenesis pathways are connected, the mechanisms by which apoB and apoE modulate HCV assembly are still poorly understood. Additionally, although it has been proposed that nascent virions travel along the Golgi apparatus, early endosomes, late endosomes, recycling endosomes, and secretory vesicles (7, 8), the mechanisms that regulate such exocytic processes have not been deciphered so far.

Clathrin mediates the sorting of membrane proteins in the endocytic and secretory pathways at the plasma membrane, endo-

somal membranes, and *trans*-Golgi network (TGN) (9). Clathrin-mediated protein transport is achieved through the action of multiple adaptors, including AP-1 and AP-2. Whereas AP-1 mediates the delivery of proteins to the plasma membrane, AP-2 is involved in endocytic processes (10). On the other hand, clathrin is essential for both the entry and secretion of some viruses into/from host cells (11–13). Although it is known that HCV entry is a clathrin-mediated process (14, 15), the possible role of clathrin in other steps of the HCV cycle has not been studied. In this study, we uncovered a role for clathrin in HCV egress. Our results suggest that AP-1 participates in HCV egress in a post-endoplasmic retic-

Received 19 December 2014 Accepted 20 January 2015

Accepted manuscript posted online 28 January 2015

Citation Benedicto I, Gondar V, Molina-Jiménez F, García-Buey L, López-Cabrera M, Gastaminza P, Majano PL. 2015. Clathrin mediates infectious hepatitis C virus particle egress. *J Virol* 89:4180–4190. doi:10.1128/JVI.03620-14.

Editor: R. W. Doms

Address correspondence to Pedro L. Majano, pedro.majano@salud.madrid.org.

* Present address: Ignacio Benedicto, Margaret Dyson Vision Research Institute, Department of Ophthalmology, Weill Cornell Medical College, New York, New York, USA.

I.B. and V.G. contributed equally to this article.

Copyright © 2015, American Society for Microbiology. All Rights Reserved.

doi:10.1128/JVI.03620-14

ulum (post-ER) compartment and that clathrin interference results in the redistribution of HCV core from early endosomes to lysosomes.

MATERIALS AND METHODS

Cell culture. The human hepatocyte-derived cell lines Huh7 (JCRB-0403) and Huh7 Lunet N (16) were grown as previously reported (17). The full-length HCV replicon-containing clone HCV-G5 was generated and cultured as previously described (17). For hepatocyte-like polarized cultures, we employed Matrigel-based three-dimensional (3D) spheroids as previously described (18), with minor modifications. One-hundred-microliter aliquots of 50% Matrigel (BD Biosciences) diluted in complete medium were deposited into either 8-well chambered cover glasses (Nalge Nunc International) or 48-well plates (Corning Incorporated) and incubated at 37°C for 30 min. Cells were plated on top of the gel and processed as indicated. Hepatocyte-like polarity was confirmed by immunofluorescence and confocal microscopy analyses as described previously (18).

HCVcc infection and harvest. JFH-1 HCVcc was produced as previously described (17) and expanded in culture for several passages. For HCVcc infection of conventional cultures, 10^5 cells were seeded into 6-well plates and, 24 h later, infected at a multiplicity of infection (MOI) of 0.01. For some experiments, conditions were scaled to different plate sizes. At 3 days postinfection, the medium was changed or cells were transfected with small interfering RNAs (siRNAs) (see below). After 2 days, cells were washed and incubated in fresh medium for 6 h. Where indicated, 50 μ M Pitstop2 (Abcam), 80 μ M dynasore, or 1 μ M brefeldin A (BFA) (Sigma) was added during the indicated time before processing of cells and supernatants. The Pitstop2 dose was chosen based on the 50% inhibitory concentration (IC_{50}) (~ 15 μ M) for transferrin internalization inhibition (19). The dynasore and BFA doses employed here have been used successfully previously (5, 20). 3D-cultured cells were infected as previously described (18).

HCVcc production in Huh7 Lunet N cells. A total of 4×10^6 Huh7 Lunet N cells were electroporated with 5 μ g JFH-1 RNA at 975 μ F and 270 V as previously described (17) and then seeded into 10-cm dishes. After 24 h, cells were trypsinized and reseeded in 6-well plates (3×10^5 cells per well). For pharmacological inhibition experiments, cells were treated 2 days after reseeding, and HCVcc was collected as described above. For siRNA experiments, cells were transfected with the indicated siRNAs 8 h after reseeding, and HCVcc was harvested 2 days later, as described above. For immunofluorescence assays, cells were reseeded on coverslips, fixed or lysed 2 days after siRNA transfection, and processed as described below.

siRNA transfection. Cells were transfected at 3 days postinfection with 200 nM ON-TARGETplus SMARTpool siRNAs against the human clathrin heavy chain (CHC), the AP-1 gamma subunit (AP1G1), the AP-2 medium subunit (AP2M1), apoB, or apoE. Alternatively, cells were transfected with individual siRNAs (200 nM) against the clathrin heavy chain. Control cells were transfected with the same amount of ON-TARGETplus nontargeting pool or a single control siRNA (Dharmacon). siRNAs and 4 μ l Dharmafect 1 (Dharmacon) were diluted in 0.75 ml antibiotic-free Opti-MEM I (Gibco) in separate tubes. After a 5-min incubation at room temperature, both dilutions were mixed and incubated for an additional 20 min at room temperature. The transfection mix was then supplemented with 10% fetal calf serum and added to cells grown in 6-well plates. For some experiments, conditions were scaled to different plate sizes. After an overnight incubation at 37°C, the transfection mix was replaced with complete medium. Two days after transfection, knockdown efficiency was determined by Western blotting, and cells and supernatants were processed as indicated.

Determinations of HCV RNA level and infectivity. For intracellular HCV RNA quantification, RNA extraction, reverse transcription (RT), and real-time PCR were performed as previously described (17). Extracellular HCV RNA was measured similarly, but employing TRIzol LS reagent (Ambion) for RNA extraction and adding an overnight RNA precipitation step at -20°C in the presence of 20 μ g of glycogen (Roche).

Intracellular infective particles were extracted by four freeze-thaw cycles as previously described (21). Titrations of both extracellular and intracellular infectivities were carried out by infection of 2×10^4 Huh7 cells grown in 48-well plates with diluted supernatants and lysates, respectively, followed by RNA extraction at 3 days postinfection, RT, and real-time PCR.

Western blots and ELISAs. Western blotting was carried out as previously described (17), using the following antibodies: rabbit anti-clathrin heavy chain, mouse anti-alpha 1 antitrypsin (anti- α 1AT), rabbit anti-LAMP1 (Abcam), rabbit anti-EEA1 (Cell Signaling Technology), mouse anti-p53, mouse anti-HCV core (C7-50) (Santa Cruz Biotechnology), mouse anti-AP1G1, mouse anti-AP50 (AP-2 medium subunit) (BD Transduction Laboratories), goat anti-apoB, and goat anti-apoE (Calbiochem). Human apoB and apoE enzyme-linked immunosorbent assay (ELISA) kits (Abnova) were used as recommended by the manufacturer, using supernatants from siRNA- or inhibitor-treated cells that were harvested as described above.

Immunofluorescence analysis. Cells were grown on coverslips or Matrigel and infected as described above. Transfection with siRNAs was performed where indicated. Immunofluorescence and confocal microscopy analyses were carried out as previously described (17), employing antibodies against ZO-1 (Life Technologies), HCV core, EEA1, LAMP1, AP1G1, and apoE. The secondary antibodies used were Alexa 488-conjugated goat anti-rabbit or donkey anti-goat and Alexa 647-conjugated goat anti-mouse antibodies (Molecular Probes, Inc.). For multiple stainings, samples were incubated sequentially with the indicated primary and secondary antibodies. Transferrin receptor was detected with a fluorescein isothiocyanate (FITC)-labeled mouse anti-transferrin receptor (BD Transduction Laboratories). Confocal microscopy was performed with a Leica TCS SP5 laser scanning system (Leica Microsystems). For colocalization studies, five x - y optical sections spaced by 0.6 to 0.8 μ m in the z axis were acquired from 20 cells (two independent experiments with 10 cells each). Mander's overlap coefficients for the whole stack of each cell (fraction of HCV core that colocalized with the AP-1, apoE, EEA1, or LAMP1 signal) were analyzed using the ImageJ JACoP plug-in (22) and plotted with Graph Pad Prism software.

Proliferation assays. Huh7 cells were grown overnight in 96-well plates and transfected with control, CHC, or AP-1 siRNAs. Forty-eight or 72 h later, MTT [3-(4,5-dimethyl-2-thiazolyl)-2,5-diphenyl-2H-tetrazolium bromide; Sigma, St. Louis, MO] was added to a final concentration of 0.5 mg/ml in complete RPMI 1640 medium without phenol red. After 3 h of incubation at 37°C, the medium was removed, and 100 μ l 0.1 N HCl in absolute isopropanol was added to each well. The absorbance at 570 nm was measured in a Sunrise Basic Tecan ELISA reader (Tecan Austria GmbH, Grödig, Austria), and values were interpolated into a standard curve.

Immunoprecipitation. Protein G Sepharose (GE Healthcare Bio-Sciences AB) was washed three times with phosphate-buffered saline (PBS) and resuspended in PBS to obtain a 50% slurry. Anti-apoB, anti-apoE (Calbiochem), or control goat IgG (Santa Cruz Biotechnology) was incubated with the 50% slurry for 30 min at room temperature, with mixing, at a concentration of 2.5 μ g antibody per 100 μ l 50% slurry. Unbound antibodies were removed by washing three times with cold PBS, and PBS was added to obtain the antibody-bound 50% slurry. Supernatants and detergent-free lysates obtained from 6-well plates were diluted 1/5 in complete medium and precleared with 100 μ l 50% slurry for 1 h at 4°C, with mixing. Triplicate aliquots of precleared supernatants or lysates were used to determine the level of input HCV RNA. Immunoprecipitation was carried out by incubating 0.5 ml precleared supernatant or lysate with 40 μ l antibody-bound 50% slurry for 3 h at 4°C, with mixing. Postimmunoprecipitation supernatants or lysates were used for titration experiments, and immunoprecipitates were washed three times with cold complete medium and processed for Western blotting or HCV RNA determination by using TRIzol LS reagent and glycogen for RNA precipitation (see above).

Statistical analysis. Homoscedasticity and normal distribution were tested and comparison of means analyzed by using one-way analysis of variance (ANOVA). The Mann-Whitney U test was used under violated assumptions. All analyses were performed with G-Stat 2.0 software. *P* values of ≤ 0.05 , ≤ 0.01 , and ≤ 0.001 are represented by asterisks (*, **, and ***, respectively) in the figures.

RESULTS

HCVcc egress is mediated by clathrin, AP-1, and dynamin. We first addressed whether clathrin and AP-1 are involved in HCVcc secretion. Huh7 cells were infected with HCVcc at an MOI of 0.01, and at 3 days postinfection, cells were transfected with siRNA pools specific for either CHC or the AP-1 gamma subunit. After 2 days, cells were extensively washed and incubated with fresh medium for six additional hours. Extracellular HCV RNA levels and infectivity were significantly reduced after CHC and AP-1 knockdown, whereas intracellular HCV levels were not significantly altered (Fig. 1A and B). Similar results were obtained using four different individual siRNAs against CHC (Fig. 1C and D). We noted that CHC and AP-1 knockdown did not induce any alteration in cell proliferation or HCV RNA replication (Fig. 1E and F). Furthermore, we observed no reduction in either HCV core expression levels or the number of viral protein-positive cells after CHC or AP-1 knockdown at the time point when cells and supernatants were processed (Fig. 1G and H), strongly suggesting that the differences observed in extracellular infectivity and HCV RNA levels were not due to a reduction of viral replication or an impaired spread of infection caused by a block of HCVcc entry. To further support this notion, we studied the roles of clathrin and AP-1 in HCVcc egress by using Huh7 Lunet N cells (16), into which HCV RNA was introduced by electroporation. These cells are able to secrete infective virions but are resistant to secondary infection due to the lack of the HCV coreceptor CD81 (16). Thus, they constitute an ideal tool for studying HCVcc exocytosis in a single round of viral egress. In agreement with the results obtained with Huh7 cells, CHC and AP-1 knockdown impaired HCVcc egress without affecting intracellular viral RNA and infectivity levels (Fig. 1I).

Next, we employed a pharmacological approach to study whether acute clathrin inhibition impaired HCV exocytosis. Treatment of HCVcc-producing Huh7 Lunet N cells with the clathrin inhibitor Pitstop 2 (19) significantly reduced HCVcc secretion without altering intracellular viral levels (Fig. 2A). We also assessed the role of dynamin in HCV egress. Dynamin is a GTPase essential for membrane fission events during several cellular processes that involve vesicle formation (23). Although dynamin's best-studied function is its role during clathrin-mediated endocytosis, it has also been shown to participate in trafficking from the TGN (24). Dynamin inhibition by dynasore treatment (25) significantly impaired HCVcc egress without reducing intracellular viral levels (Fig. 2A). Since HCV entry is a clathrin-dependent process, we wanted to rule out the possibility that the reduced extracellular infectivity of inhibitor-treated cells was an artifact due to the impaired viral entry during titration experiments caused by inhibitor carryover. Although it was very unlikely, we considered the most extreme scenario and assumed that 100% of inhibitor activity was still present in HCVcc-containing supernatants after their harvest. We performed infection experiments by adding 2.5 μ M Pitstop 2 or 4 μ M dynasore to HCVcc-containing supernatants that were generated by infected Huh7 cells in the

absence of inhibitors. The concentrations used were 20-fold lower than those applied to HCVcc-producing cells (50 μ M Pitstop 2 and 80 μ M dynasore), since titration experiments were routinely carried out using a 1:20 dilution of infective supernatants. Under these conditions, we observed no impairment of HCVcc infection (Fig. 2B), thus demonstrating that the effects shown in Fig. 2A were not due to inhibitor carryover but to defective HCVcc secretion from inhibitor-treated cells. The impairment of HCVcc egress by Pitstop 2 and dynasore treatment was confirmed in 3D cultures of hepatocyte-like polarized Huh7 cells (Fig. 2C to E), which were previously described by our group (18).

The fact that both CHC and AP-1 depletions resulted in similar blocks of virus production suggested that clathrin-mediated anterograde transport was involved in HCVcc egress. However, in order to confirm that the effects mediated by CHC or dynamin knockdown and/or inhibition were not due to defective endocytic processes, we performed the same set of experiments by knocking down the medium subunit of the clathrin adaptor AP-2, a well-defined complex that regulates endocytosis of certain plasma membrane proteins (10) and has been shown to be essential for endocytic clathrin-coated pit and clathrin-coated vesicle formation (26, 27). Whereas AP-2 knockdown effectively impaired transferrin receptor internalization (Fig. 3A and B), extracellular HCV RNA levels were not reduced (Fig. 3C). Although this result did not rule out a role of AP-2 in viral particle assembly (see Discussion), it indicated that viral exit from infected cells was not compromised after AP-2 knockdown. Collectively, these data strongly suggest that HCVcc egress depends on exocytic transport routes that require the concerted action of clathrin, AP-1, and dynamin.

apoB and apoE secretion is not impaired after clathrin interference. Since HCV exit from cells has been proposed to be tightly linked to VLDL secretion (1), we next sought to determine whether the impairment of HCV egress observed after perturbing clathrin-mediated trafficking could be due to a defective exocytosis of VLDL-associated proteins. Employing the same experimental approaches as those described above, we tested the effects of clathrin and AP-1 knockdown and/or pharmacological inhibition on apoB and apoE secretion from infected cells. Interestingly, in contrast to HCV egress, ELISAs and Western blot analyses showed no significant reduction in apoB and apoE secretion after clathrin or AP-1 knockdown and/or inhibition in both Huh7 cells (Fig. 4A to C) and Huh7 Lunet N cells (data not shown). To further confirm that clathrin inhibition did not impair apoB and apoE secretion, we performed kinetic assays and observed that the Pitstop 2-induced reduction in viral RNA egress was not paralleled by a decrease in apoB or apoE secretion at any time point studied (Fig. 4D and E). In contrast, dynamin inhibition impaired both apoB and apoE exocytosis (Fig. 4C). These results were confirmed in 3D cultures of hepatocyte-like polarized Huh7 cells (Fig. 2F and G). We noted that dynasore treatment also prevented α 1AT secretion, possibly indicating a broader role of dynamin in general exocytic processes.

Altogether, these data suggested that whereas HCVcc egress was a clathrin-, AP-1-, and dynamin-dependent process, secretion of VLDL-associated proteins was mediated by dynamin but not by clathrin or AP-1. In agreement with previous reports, apoB (5) and apoE (3) knockdown inhibited HCVcc assembly and egress without altering intracellular HCV RNA levels (data not shown). Hence, these results indicated that whereas apoB and apoE down-

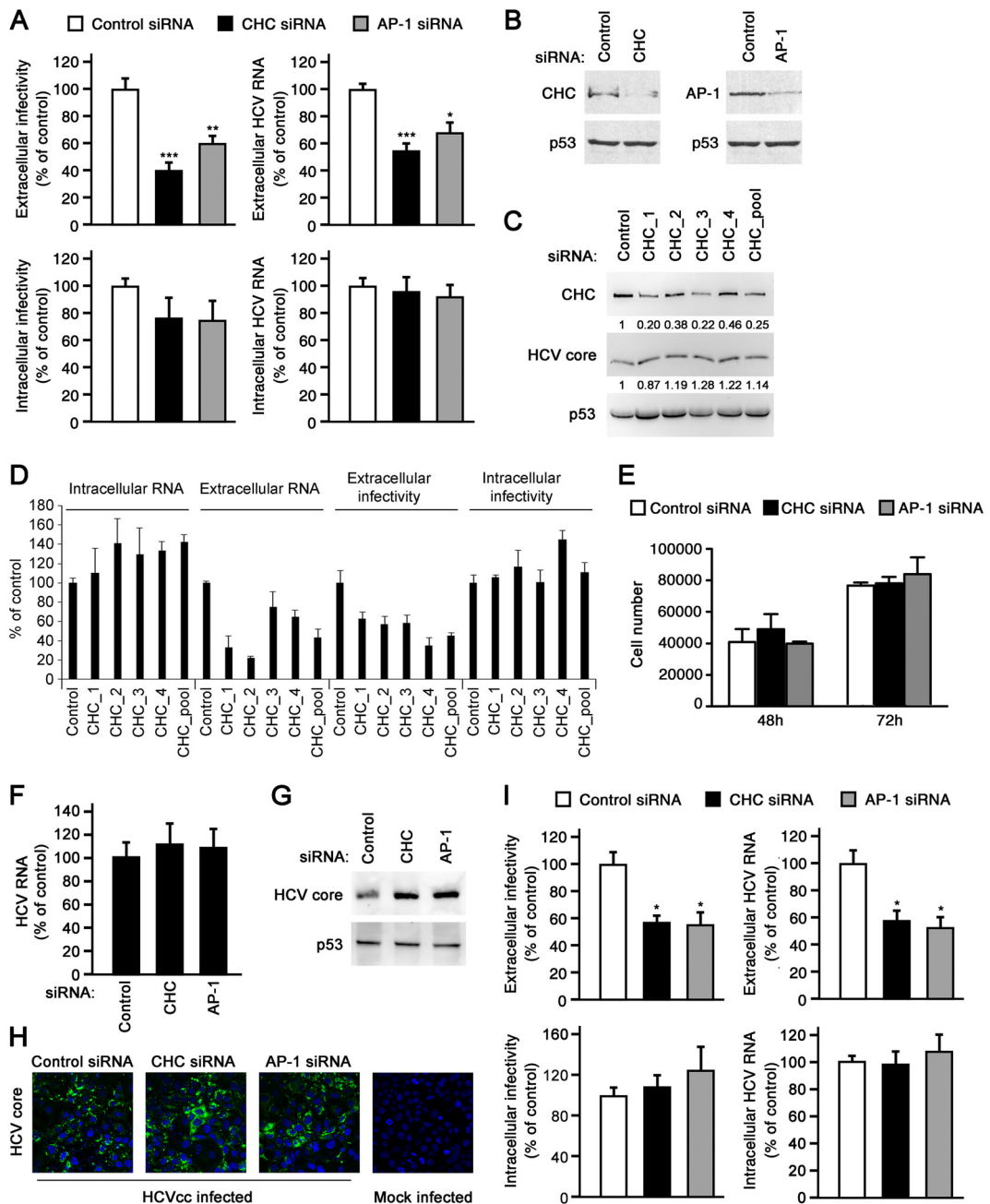


FIG 1 HCVcc egress is mediated by clathrin and AP-1. (A) HCV RNA and infectivity quantification after CHC and AP-1 knockdown in infected Huh7 cells. Results are expressed as means and standard errors of the means (SEM) for at least three experiments performed in triplicate. (B) Western blot analysis of CHC and AP-1 knockdown efficiencies in Huh7 cells. p53 was used as a loading control. (C) Western blot analysis of HCV core protein levels and CHC knockdown efficiency after transfection of HCVcc-infected Huh7 cells with either control siRNA, four different CHC-specific siRNAs, or the pooled CHC siRNA mix used for panel B. p53 was used as a loading control. Numbers indicate the relative intensities of bands compared to those for control cells after being normalized to p53 levels. (D) HCV RNA and infectivity quantification after CHC knockdown. Results are expressed as means and SEM for an experiment performed in triplicate. (E) Cell proliferation was assessed as described in Materials and Methods. Results obtained 48 h and 72 h after transfection are shown. (F) HCV RNA levels in a clone containing a full-length HCV replicon were analyzed by real-time RT-PCR. (G) HCV core levels were analyzed by Western blotting. p53 was used as a loading control. (H) HCV core levels were analyzed by immunofluorescence. Green, HCV core; blue (DAPI [4',6-diamidino-2-phenylindole]), nuclei. (I) HCV RNA and infectivity quantification after CHC and AP-1 knockdown in HCVcc-producing Huh7 Lunet N cells. Results are expressed as means and SEM for at least three experiments performed in triplicate.

regulation was detrimental for HCVcc morphogenesis and secretion, the decrease in HCV egress observed after clathrin or AP-1 interference was not due to an impairment of the main exocytic route followed by these VLDL-associated proteins.

Participation of apoE and AP-1 at different points along the HCVcc secretory pathway. Our results suggested that HCV hijacked both the VLDL assembly pathway and clathrin-mediated anterograde traffic during viral egress. However, we found no ev-

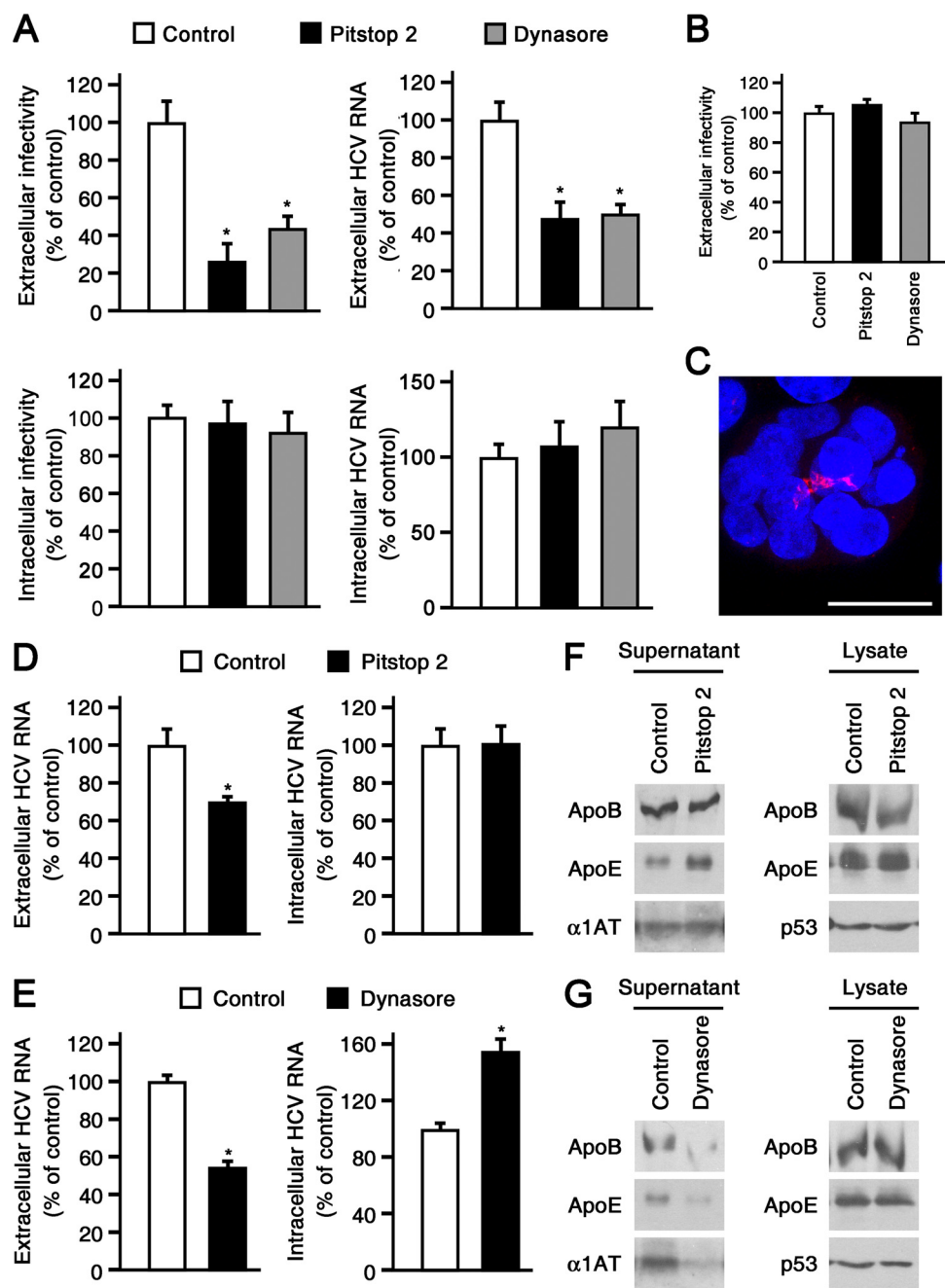


FIG 2 HCVcc secretion is impaired after clathrin and dynamin pharmacological inhibition. (A) HCV RNA levels after clathrin or dynamin inhibition in Huh7 Lunet N cells by 50 μ M Pitstop 2 or 80 μ M dynasore treatment, respectively. Data are presented relative to those for vehicle-treated control cells. Results are expressed as means and SEM for four experiments performed in triplicate. (B) Analysis of the possible effects of Pitstop 2 and dynasore carryover during titration of infective supernatants after inhibitor treatment. (C) Polarized hepatocyte-like localization of ZO-1 in Huh7 cells cultured on Matrigel. Red, ZO-1; blue (DAPI), nuclei. Bar, 25 μ m. (D and E) Effects of Pitstop 2 (D) or dynasore (E) treatment on extracellular and intracellular HCV RNA levels in 3D-cultured, HCVcc-infected Huh7 cells. Results are presented relative to those for vehicle (dimethyl sulfoxide [DMSO])-treated control cells and are expressed as means and SEM for three experiments. (F and G) Western blot analyses of apoB and apoE levels in supernatants and cellular lysates obtained from 3D-cultured, HCVcc-infected Huh7 cells after clathrin (F) or dynamin (G) inhibition. α 1AT and p53 were used as loading controls.

idence supporting a role of clathrin or AP-1 in apoB or apoE exocytosis. Thus, we hypothesized that HCVcc egress may share some steps with both VLDL assembly and clathrin-mediated trafficking, but at different points along the secretory pathway. First, given the controversy regarding apoB association with HCVcc, we wanted to study HCVcc apolipoprotein composition in our ex-

perimental system. As shown in Fig. 5A to C, apoE but not apoB was clearly detected as part of the infective viral particle, similar to previously published data (6, 28). In order to determine the sub-cellular location of HCVcc and apoE association, we next performed a series of immunoprecipitation experiments using cell lysates obtained by repeated freeze-thaw cycles. We employed this

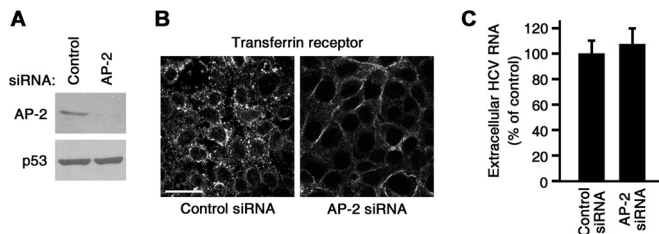


FIG 3 HCV exocytosis is not mediated by AP-2. (A) Western blot analysis of AP-2 knockdown efficiency. p53 was used as a loading control. (B) Immunofluorescence analysis of transferrin receptor localization after AP-2 knockdown. Bar, 25 μ m. (C) HCVcc-infected cells were transfected with control or AP-2-specific siRNAs, and HCV RNA levels in supernatants were quantified by real-time RT-PCR. Results are presented relative to those for control siRNA-transfected cells and are expressed as means and SEM for six experiments performed in triplicate.

detergent-free approach to avoid the possible envelope removal from the intracellular viral particle (29). As shown in Fig. 5D, HCV RNA clearly coimmunoprecipitated with apoE above background levels. In addition, apoE knockdown caused a marked decrease in the level of coimmunoprecipitated HCV RNA with the anti-apoE antibody (Fig. 5D). Note that the amount of the cellular histone H3 RNA that coimmunoprecipitated with apoE was indistinguishable from background levels, regardless of apoE knockdown (Fig. 5D). These results indicated that HCV RNA specifically coimmunoprecipitated with intracellular apoE. Next, we repeated these experiments but treated cells with brefeldin A (BFA), a drug that inhibits ER-to-Golgi traffic (30). As previously reported (5), BFA treatment of infected cells caused marked reductions in secreted HCV RNA and extracellular infectivity, which were accompanied by \sim 2-fold increases in both intracellular viral RNA and infectivity (Fig. 5E). Interestingly, detergent-free immunoprecipitation assays after BFA treatment showed a

proportional accumulation of intracellular apoE-associated HCV RNA (Fig. 5F, left panel). Importantly, intracellular infectivity of BFA-treated cells was reduced after apoE immunoprecipitation (Fig. 5F, right panel), suggesting that apoE was associated with infectious HCV precursors in ER-related compartments. This notion was supported by the neutralization of intracellular HCV virions from BFA-treated cells with an anti-apoE antibody previously shown to partially block HCVcc infection (4) (Fig. 5G). These results strongly suggested that apoE interaction with the virion occurred, at least in part, before it left the ER, as previously postulated by others (1).

We next sought to determine whether clathrin-mediated traffic participated in HCV egress before or after the virion exited the ER. To that end, we treated HCVcc-producing Huh7 Lunet N cells with BFA and performed immunofluorescence assays to study the colocalization between HCV core and AP-1. A similar imaging approach was used previously to assess the impact of inhibiting endosomal movement on HCVcc secretion (7). Since BFA treatment induces the accumulation of secreted cargoes in the ER, we hypothesized that if the nascent virion interacted with AP-1 before exiting the ER, blocking ER-to-Golgi traffic by BFA treatment would induce the accumulation of AP-1-positive viral particles in the ER, resulting in an increased colocalization between core and AP-1. On the other hand, if the virion interacted with AP-1 in a post-ER compartment, BFA treatment would prevent the exit of the virion from the ER, thus precluding its interaction with AP-1. Interestingly, BFA treatment resulted in a decreased colocalization between core and AP-1 (Fig. 6A), suggesting that the interaction of AP-1 with the viral particle takes place in a post-ER compartment. Conversely, BFA induced an increase in the colocalization between core and apoE (Fig. 6B). This result is in agreement with the data shown in Fig. 5F and G indicating that the interaction between apoE and the nascent virion takes place be-

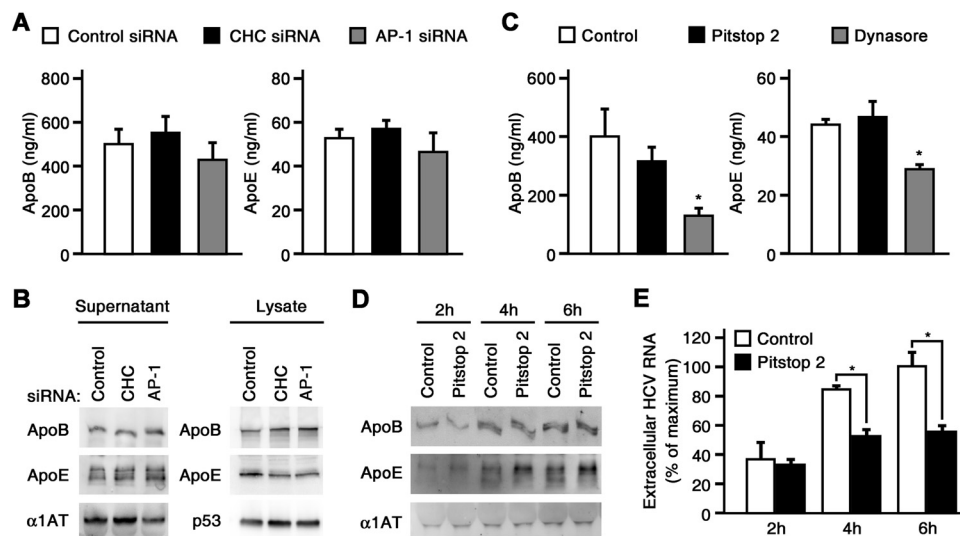


FIG 4 apoB and apoE secretion is not impaired by clathrin or AP-1 interference. (A and B) apoB and apoE levels were determined by ELISA (A) and Western blotting (B) after CHC or AP-1 knockdown in infected Huh7 cells. α 1AT and p53 were used as loading controls. (C) apoB and apoE levels in the supernatants of infected Huh7 cells after 50 μ M Pitstop 2 or 80 μ M dynasore treatment were determined by ELISA. Results are expressed as means and SEM for two experiments performed in duplicate. (D and E) Kinetic analyses of secreted apoB, apoE, and α 1AT (D) and of secreted HCV RNA (E) by Western blotting and real-time RT-PCR, respectively, after Pitstop 2 treatment of infected Huh7 cells. Results in panel E are presented relative to the maximum value and expressed as means and SEM for three experiments.

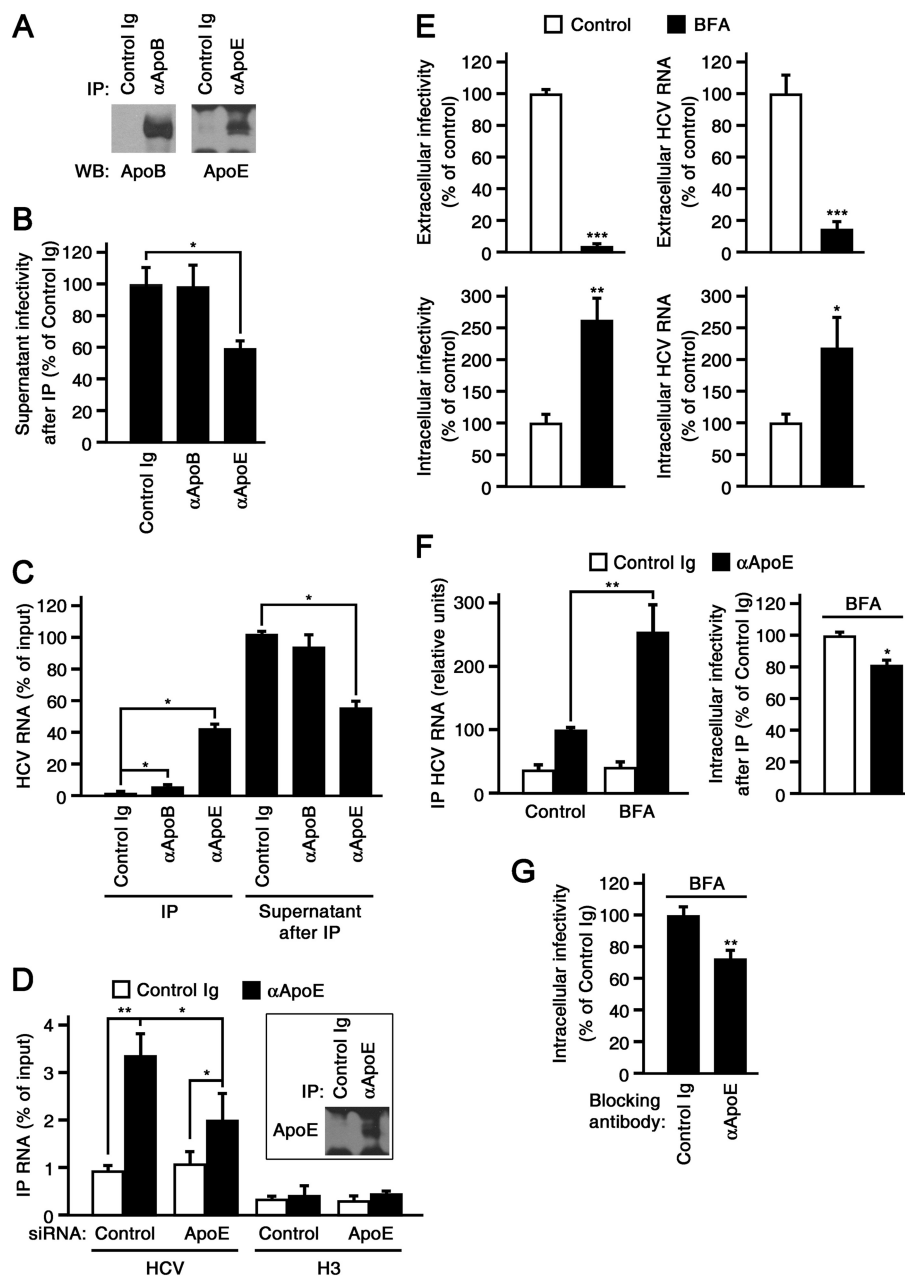


FIG 5 Intracellular HCVcc-apoE association in BFA-treated cells. (A) Immunoprecipitation (IP) from supernatants of HCVcc-infected cells, using control, anti-apoB, and anti-apoE antibodies. apoB and apoE levels were determined by Western blotting (WB). (B) Supernatant infectivity after immunoprecipitation was analyzed by titration on Huh7 cells and real-time RT-PCR. Results are presented relative to the infectivity of control Ig-immunoprecipitated supernatants and are expressed as means and SEM for three experiments. (C) Supernatant immunoprecipitation was carried out as described for panels A and B, and RNAs were extracted from both immunoprecipitates and postimmunoprecipitation supernatants. HCV RNA levels were assessed by real-time RT-PCR and presented as percentages of input HCV RNA. Results are expressed as means and SEM for three experiments. (D) Immunoprecipitates from detergent-free lysates of HCVcc-infected, siRNA-transfected cells were used for either Western blot analysis (inset; control siRNA-transfected cells) or HCV RNA quantification. (E) HCV RNA levels and infectivities after 1 μ g/ml BFA treatment. (F) (Left) Immunoprecipitated HCV RNA levels after BFA treatment. (Right) Intracellular infectivities of BFA-treated cells after immunoprecipitation. (G) Intracellular infectivities of BFA-treated cells, assessed by titration on Huh7 cells in the presence of 5 μ g/ml control or anti-apoE antibody. Results are expressed as means and SEM for at least three experiments.

fore its exit from the ER. Collectively, these results suggest that apoE and AP-1 interact with the nascent virion before and after its exit from the ER, respectively.

Clathrin and AP-1 knockdown alters HCV core endosomal localization. Our data suggested that interfering with clathrin-mediated anterograde trafficking could block viral egress at the

level of a post-ER compartment. However, we did not detect an increase in intracellular infectivity after CHC or AP-1 knockdown (Fig. 1). What happens, then, with the nonsecreted viral particles? It has been shown that newly formed immature HCVcc particles are actively degraded in a post-ER cellular compartment and that only mature, low-density particles escape degradation and un-

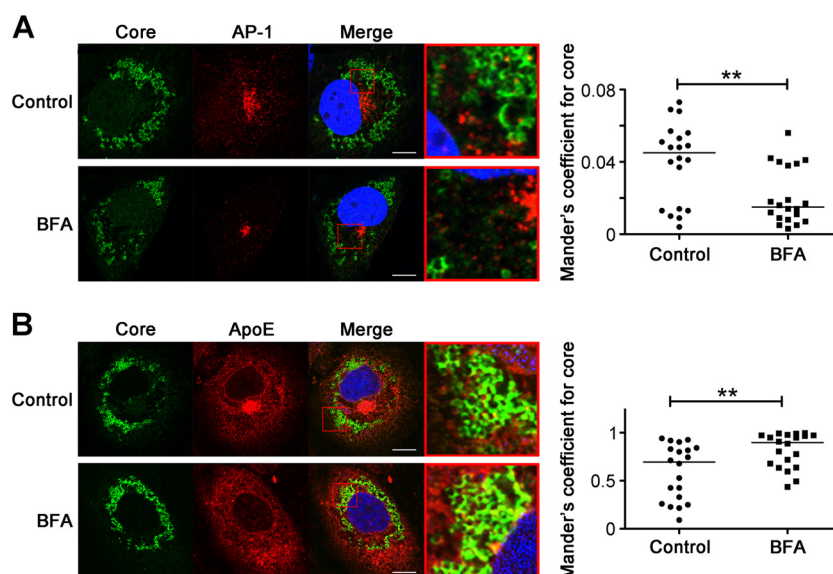


FIG 6 Colocalization of HCV core with AP-1 and apoE after BFA treatment. HCVcc-producing Huh7 Lunet N cells were treated with 1 μ g/ml BFA for 6 h and fixed for further immunofluorescence analysis. Green, HCV core; red, AP-1 (A) or apoE (B); blue (DAPI), nuclei. Images show a single x - y section from the confocal stack of a representative cell. The red box shows a detail of the merged image. Bars, 10 μ m. In the scatterplots, each dot represents Mander's coefficient for HCV core (fraction of HCV core that colocalizes with AP-1 or apoE) for each of the 20 cells from two independent experiments (see Materials and Methods for details). The horizontal lines represent median Mander's coefficients for all cells studied.

dergo exocytosis (5). Thus, we hypothesized that if the exocytic route followed by mature viral particles was blocked by interfering with clathrin-mediated trafficking, those virions could be diverted toward degradation, possibly at the lysosomes. Since inhibition of endosomal movement results in the accumulation of HCV core at early endosomes and in impaired viral secretion, it has been proposed that HCV particles traffic through early endosomes before exiting the cell (7). Thus, we studied the colocalization of HCV core and either the early endosome marker EEA1 or the lysosome marker LAMP1 after CHC or AP-1 knockdown in HCVcc-producing Lunet N cells. As shown in Fig. 7A, both CHC and AP-1 knockdowns induced decreases in the colocalization between HCV core and EEA1. Conversely, CHC or AP-1 knockdown resulted in increased colocalization between the viral protein and LAMP1. Note that CHC or AP-1 knockdown did not alter HCV core, EEA1, or LAMP1 protein levels as determined by Western blotting (Fig. 7B). These results demonstrated that clathrin and AP-1 knockdown impaired the normal endosomal localization of HCV core, suggesting an altered transendosomal exocytic HCVcc pathway that results in the lysosomal disassembly of some of the mature viral progeny.

DISCUSSION

Herein we demonstrated a role for clathrin and its adaptor AP-1 in HCVcc egress, which could not be attributed to impaired apoE or apoB secretion. In addition, biochemical and imaging experiments suggested that apoE and AP-1 participate in HCVcc egress at different points along the secretory pathway, with AP-1 being involved in a post-ER transendosomal route that enables the virion to exit the cell, escaping from lysosomal disassembly.

Several studies have followed knockdown approaches to assess the roles of clathrin and its adaptors in protein sorting (31–33). Notably, the magnitudes of the effects observed did not quantitatively match the strong knockdown efficiencies achieved. Simi-

larly, the impairment of HCV egress we detected after clathrin or AP-1 interference was moderate. This can be explained by the fact that residual amounts of the knocked-down protein may be sufficient to partially enable the studied process. Alternatively, as shown for LDL uptake in lipoprotein-starved AP-2-depleted cells (26, 27), inhibition of a trafficking pathway might lead to the acquisition of a surrogate route, which may partially mask the experimental readout. Nevertheless, our results obtained following different approaches to interfere with clathrin and AP-1 (siRNA and chemical inhibition) in several culture systems (Lunet N and 2D- and 3D-cultured Huh7 cells) were consistent, strongly suggesting a role for clathrin and AP-1 in HCV exocytosis.

The aforementioned reports (31–33) showed that in polarized epithelial cells, clathrin and AP-1 participate in trafficking pathways followed by basolateral membrane proteins from both the TGN and recycling endosomes to the plasma membrane. Thus, it is plausible that nascent virions interact with such a protein within the cell *en route* to the plasma membrane, during either biosynthetic or recycling transport, to facilitate viral egress. Interestingly, knockdown approaches and live-cell imaging experiments have suggested that both TGN and recycling endosome proteins mediate HCV exocytosis (8). Additionally, depletion of the Golgi-specific phosphatidylinositol 4-phosphate pool has been shown to impair HCV secretion (34). Although our data suggest that the involvement of AP-1 in HCV egress takes place in a post-ER compartment, further studies will be needed to more precisely address the subcellular compartment(s) where clathrin exerts its role in HCV exocytosis and to investigate the possible participation of a cellular protein as a “carrier” during viral secretion.

There are several examples in the literature showing that perturbation of the traffic routes followed by different cellular proteins can impair viral egress and induce the accumulation of viral structural proteins in lysosomal compartments. Inhibition of N-glycan process-

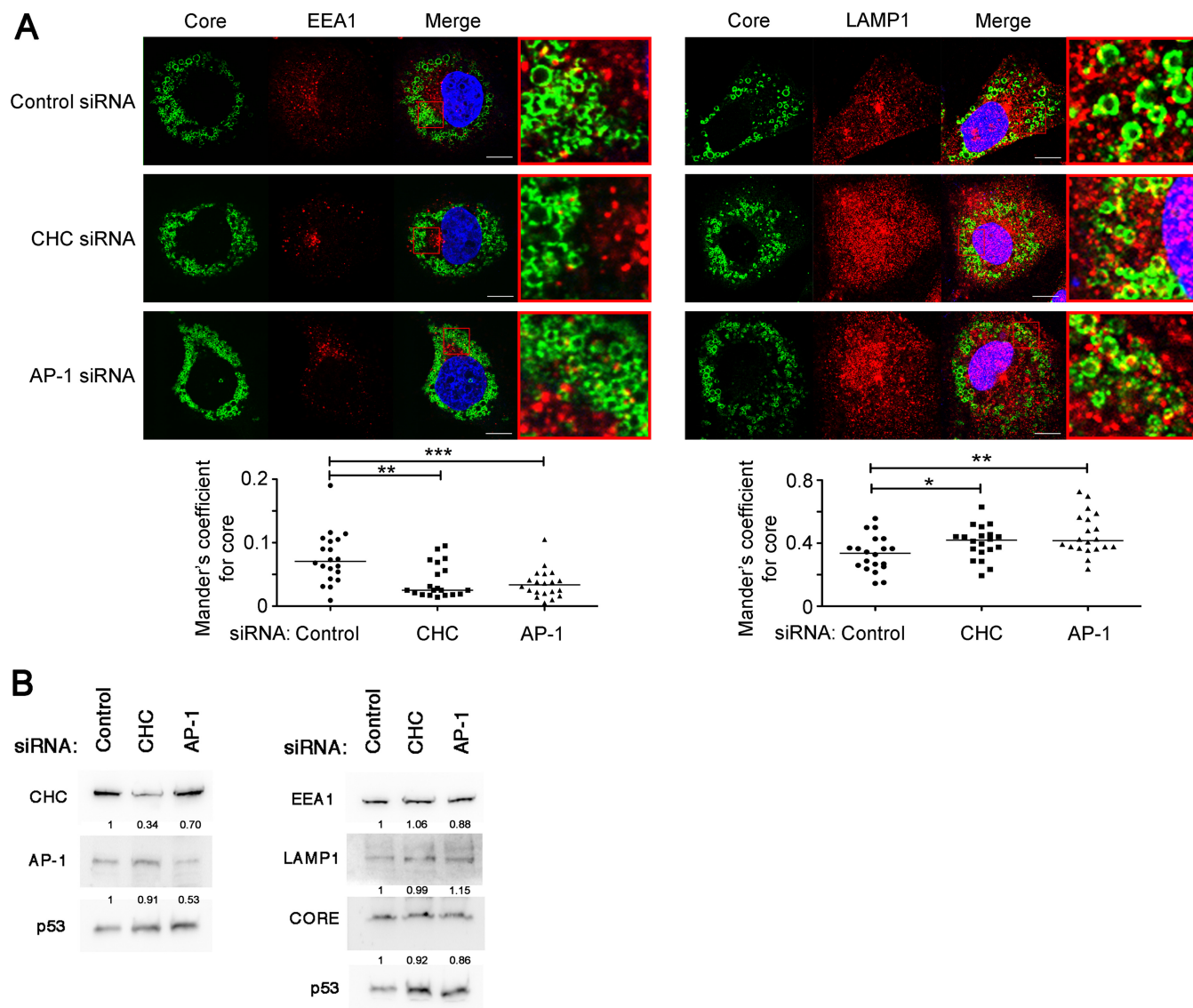


FIG 7 Colocalization of HCV core with EEA1 and LAMP1 after CHC or AP-1 knockdown. (A) HCVcc-producing Huh7 Lunet N cells were transfected with control, CHC, or AP-1 siRNAs and fixed 2 days later for immunofluorescence analysis. Green, HCV core; red, EEA1 (left) or LAMP1 (right); blue (DAPI), nuclei. Images show a single x - y section from the confocal stack of a representative experiment. The red box shows a detail of the merged image. Bars, 10 μ m. Quantification and scatterplot representations were performed as described in the legend to Fig. 6 and in Materials and Methods. (B) (Left) Western blot showing efficiency of CHC or AP-1 knockdown. (Right) Western blot showing unaltered expression levels of EEA1, LAMP1, and core after CHC or AP-1 knockdown. Numbers indicate the relative intensities of bands compared to those of control cells after being normalized to p53 levels.

ing, which results in the defective trafficking and secretion of certain glycoproteins, was shown to inhibit viral DNA secretion and to induce the accumulation of hepatitis B virus structural proteins within lysosomal compartments (35). Another interesting example is Niemann-Pick type C-1-deficient cells, in which cholesterol and cellular proteins accumulate in late endosomal/lysosomal compartments. After human immunodeficiency virus type 1 infection, the viral capsid protein fails to traffic properly and also accumulates within these compartments, resulting in a decreased release of infectious particles (36). In this context, one possibility is that the lysosomal accumulation of HCV core after CHC or AP-1 knockdown represents a failure of HCVcc assembly, with the viral protein reaching the lysosome before being assembled into the capsid of a nascent virion. However, the fact that blocking ER-to-Golgi traffic by BFA

treatment induces the intracellular accumulation of infective viral particles strongly suggests that capsid assembly takes place before the virion exits the ER. Since AP-1 is localized at the TGN and recycling endosomes (i.e., post-ER compartments) and AP-1 colocalization with HCV core is reduced upon BFA treatment, it is not likely that AP-1 knockdown interferes with HCV capsid assembly. Another possibility is that lysosomal HCV core accumulation after CHC or AP-1 interference represents an endpoint of the nascent virion after being diverted from the TGN or recycling endosomes during its normal secretory route. Undoubtedly, live-cell imaging experiments studying HCV core trafficking (8) would be very helpful for testing these hypotheses. Additionally, elucidating the cellular exocytic trafficking pathways altered after CHC or AP-1 knockdown may help to assess these and other possible scenarios.

Our data revealed the implication of clathrin in HCVcc secretion but did not rule out additional roles in the assembly process. Indeed, while our manuscript was in preparation, it was reported that the clathrin adaptor AP-2 interacts with core and participates in HCVcc assembly (37). Whereas this observation may represent a link between clathrin and HCV assembly, it seems to be contradictory with our data regarding AP-2 knockdown. However, the experimental designs of both studies were notably different. In the previous work, cells were transfected with HCV RNA after AP-2 depletion. In the present study, cells were first infected and then transfected with AP-2 siRNA after allowing infection to spread, so it is possible that the presence of assembled virions prior to the reduction of AP-2 levels masked assembly defects induced by AP-2 knockdown. In conclusion, while our experiments did not show evidence against a role for AP-2 in HCVcc assembly, they suggest that AP-2 is not involved in the exocytosis of assembled virions and that clathrin-mediated HCVcc egress is not dependent on AP-2.

To date, the observed interaction between HCV and apolipoproteins both *in vitro* and *in vivo* has led to the hypothesis that HCV may use the VLDL secretory pathway to exit infected cells. However, our data showing that clathrin and AP-1 interference prevented HCVcc exocytosis but not apoB and apoE secretion raise certain doubts about the currently proposed model. Our results suggest that once the HCV virion is associated with apoE during its assembly, there is some point along the exocytic route at which lipovirion egress diverges from normal apoE secretion. Since apoE is a glycosylated protein (38), and given the key role of glycosylation during polarized exocytosis of certain membrane and soluble proteins (39), it is possible that the virion interaction with apoE modifies or masks its glycosylation pattern, thus altering its normal secretory route. Alternatively, it can also be hypothesized that viral envelope proteins may direct HCV egress through interactions with a carrier factor (see above), diverting virus-associated apolipoproteins from their natural exocytic pathway. It is worth noting that the amount of virus-associated apoE would probably be very low compared to that of total secreted apolipoprotein, in such a way that the reduction of apolipoprotein secretion caused by the block of lipovirion egress would presumably be undetectable.

We also point out that clathrin involvement in viral spread might result in cellular alterations that may lead to pathological disorders. It has been reported that mammalian reovirus infection induces clathrin recruitment to viral factories, disrupting cellular functions such as clathrin-dependent endocytosis and secretion (40). As the authors of that study argued, inhibition of clathrin-mediated trafficking routes might impair some aspects of the innate and adaptive immune responses that depend on vesicle transport, favoring the persistence of infection. In addition, virus-induced clathrin interference may cause a loss of epithelial polarization (31) with concomitant pathological consequences, including the enhancement of viral spread (41). Regarding HCV infection, the alteration of clathrin-mediated functions still needs to be addressed. However, it is interesting that in HCV replicon-containing cells, transport of major histocompatibility complex class I molecules to the cellular surface is inhibited (42), and basolateral membrane proteins are mislocalized to the apical surface (17). Whether these observations are mediated by HCV-induced clathrin alterations warrants further investigation.

In conclusion, our results showing that clathrin and AP-1 participate in HCVcc egress contribute to the understanding of HCV pathobiology and open a potential new therapeutic avenue for fighting HCV infection.

ACKNOWLEDGMENTS

This work was supported in part by the following grants: (i) grant SAF2010-21249 from the Ministerio de Ciencia e Investigación (MCI) to M.L.-C.; (ii) grant SAF2010-19270 from the MCI to P.G.; (iii) Marie Curie Career Integration grant PCIG-9-GA-2011-293664 from the European Union 7th Framework Programme for Research to P.G.; and (iv) FEDER funds via the Spanish Government to projects PI10/00101 and PI13/00159, from the Instituto de Salud Carlos III (ISCIII) Fondo de Investigaciones Sanitarias (FIS) and the Fundación Mutua Madrileña, to P.L.M. I.B. was financially supported by Centro de Investigación Biomédica En Red de Enfermedades Hepáticas y Digestivas (CIBERehd), V.G. by FIS (PI10/00101), and F.M.-J. by ISCIII and Fundación para la Investigación Biomédica (FIB) del Hospital Universitario de la Princesa.

We express our gratitude to T. Pietschmann (Institute for Experimental Virology, TWINCORE, Hanover, Germany) for the Huh7 Lunet N cells. We also thank R. Bartenschlager, F. L. Cosset, T. Wakita, and C. M. Rice for providing us with other critical reagents and L. Vega-Piris and F. Rodríguez-Salvanes (Methodological Support Unit, Instituto de Investigación Sanitaria Princesa) for statistical analysis.

We have no conflicts of interest to report.

REFERENCES

- Bartenschlager R, Penin F, Lohmann V, Andre P. 2011. Assembly of infectious hepatitis C virus particles. *Trends Microbiol* 19:95–103. <http://dx.doi.org/10.1016/j.tim.2010.11.005>.
- Nielsen SU, Bassendine MF, Burt AD, Martin C, Pumeekchokchai W, Toms GL. 2006. Association between hepatitis C virus and very-low-density lipoprotein (VLDL)/LDL analyzed in iodixanol density gradients. *J Virol* 80:2418–2428. <http://dx.doi.org/10.1128/JVI.80.5.2418-2428.2006>.
- Hishiki T, Shimizu Y, Tobita R, Sugiyama K, Ogawa K, Funami K, Ohsaki Y, Fujimoto T, Takaku H, Wakita T, Baumert TF, Miyazaki Y, Shimotohno K. 2010. Infectivity of hepatitis C virus is influenced by association with apolipoprotein E isoforms. *J Virol* 84:12048–12057. <http://dx.doi.org/10.1128/JVI.01063-10>.
- Owen DM, Huang H, Ye J, Gale M, Jr. 2009. Apolipoprotein E on hepatitis C virus facilitates infection through interaction with low-density lipoprotein receptor. *Virology* 394:99–108. <http://dx.doi.org/10.1016/j.virol.2009.08.037>.
- Gastaminza P, Cheng G, Wieland S, Zhong J, Liao W, Chisari FV. 2008. Cellular determinants of hepatitis C virus assembly, maturation, degradation, and secretion. *J Virol* 82:2120–2129. <http://dx.doi.org/10.1128/JVI.02053-07>.
- Jiang J, Luo G. 2009. Apolipoprotein E but not B is required for the formation of infectious hepatitis C virus particles. *J Virol* 83:12680–12691. <http://dx.doi.org/10.1128/JVI.01476-09>.
- Lai CK, Jeng KS, Machida K, Lai MM. 2010. Hepatitis C virus egress and release depend on endosomal trafficking of core protein. *J Virol* 84:11590–11598. <http://dx.doi.org/10.1128/JVI.00587-10>.
- Coller KE, Heaton NS, Berger KL, Cooper JD, Saunders JL, Randall G. 2012. Molecular determinants and dynamics of hepatitis C virus secretion. *PLoS Pathog* 8:e1002466. <http://dx.doi.org/10.1371/journal.ppat.1002466>.
- Brodsky FM. 2012. Diversity of clathrin function: new tricks for an old protein. *Annu Rev Cell Dev Biol* 28:309–336. <http://dx.doi.org/10.1146/annurev-cellbio-101011-155716>.
- Robinson MS. 2004. Adaptable adaptors for coated vesicles. *Trends Cell Biol* 14:167–174. <http://dx.doi.org/10.1016/j.tcb.2004.02.002>.
- Humphries AC, Dodding MP, Barry DJ, Collinson LM, Durkin CH, Way M. 2012. Clathrin potentiates vaccinia-induced actin polymerization to facilitate viral spread. *Cell Host Microbe* 12:346–359. <http://dx.doi.org/10.1016/j.chom.2012.08.002>.
- Huang C, Chang SC, Yang HC, Chien CL, Chang MF. 2009. Clathrin-mediated post-Golgi membrane trafficking in the morphogenesis of hepatitis delta virus. *J Virol* 83:12314–12324. <http://dx.doi.org/10.1128/JVI.01044-09>.

13. Mercer J, Schelhaas M, Helenius A. 2010. Virus entry by endocytosis. *Annu Rev Biochem* 79:803–833. <http://dx.doi.org/10.1146/annurev-biochem-060208-104626>.
14. Blanchard E, Belouzard S, Goueslain L, Wakita T, Dubuisson J, Wychowski C, Rouille Y. 2006. Hepatitis C virus entry depends on clathrin-mediated endocytosis. *J Virol* 80:6964–6972. <http://dx.doi.org/10.1128/JVI.00024-06>.
15. Meertens L, Bertaux C, Dragic T. 2006. Hepatitis C virus entry requires a critical postinternalization step and delivery to early endosomes via clathrin-coated vesicles. *J Virol* 80:11571–11578. <http://dx.doi.org/10.1128/JVI.01717-06>.
16. Bitzegeio J, Bankwitz D, Hueging K, Haid S, Brohm C, Zeisel MB, Herrmann E, Iken M, Ott M, Baumert TF, Pietschmann T. 2010. Adaptation of hepatitis C virus to mouse CD81 permits infection of mouse cells in the absence of human entry factors. *PLoS Pathog* 6:e1000978. <http://dx.doi.org/10.1371/journal.ppat.1000978>.
17. Benedicto I, Molina-Jimenez F, Barreiro O, Maldonado-Rodriguez A, Prieto J, Moreno-Otero R, Aldabe R, Lopez-Cabrera M, Majano PL. 2008. Hepatitis C virus envelope components alter localization of hepatocyte tight junction-associated proteins and promote occludin retention in the endoplasmic reticulum. *Hepatology* 48:1044–1053. <http://dx.doi.org/10.1002/hep.22465>.
18. Molina-Jimenez F, Benedicto I, Dao Thi VL, Gondar V, Lavillette D, Marin JJ, Briz O, Moreno-Otero R, Aldabe R, Baumert TF, Cosset FL, Lopez-Cabrera M, Majano PL. 2012. Matrigel-embedded 3D culture of Huh-7 cells as a hepatocyte-like polarized system to study hepatitis C virus cycle. *Virology* 425:31–39. <http://dx.doi.org/10.1016/j.virol.2011.12.021>.
19. von Kleist L, Stahlschmidt W, Bulut H, Gromova K, Puchkov D, Robertson MJ, MacGregor KA, Tomilin N, Pechstein A, Chau N, Chircop M, Sakoff J, von Kries JP, Saenger W, Krausslich HG, Shupliakov O, Robinson PJ, McCluskey A, Haucke V. 2011. Role of the clathrin terminal domain in regulating coated pit dynamics revealed by small molecule inhibition. *Cell* 146:471–484. <http://dx.doi.org/10.1016/j.cell.2011.06.025>.
20. Liu S, Kuo W, Yang W, Liu W, Gibson GA, Dorko K, Watkins SC, Strom SC, Wang T. 2010. The second extracellular loop dictates occludin-mediated HCV entry. *Virology* 407:160–170. <http://dx.doi.org/10.1016/j.virol.2010.08.009>.
21. Gastaminza P, Kapadia SB, Chisari FV. 2006. Differential biophysical properties of infectious intracellular and secreted hepatitis C virus particles. *J Virol* 80:11074–11081. <http://dx.doi.org/10.1128/JVI.01150-06>.
22. Bolte S, Cordelieres FP. 2006. A guided tour into subcellular colocalization analysis in light microscopy. *J Microsc* 224:213–232. <http://dx.doi.org/10.1111/j.1365-2818.2006.01706.x>.
23. Ferguson SM, De Camilli P. 2012. Dynamin, a membrane-remodelling GTPase. *Nat Rev Mol Cell Biol* 13:75–88. <http://dx.doi.org/10.1038/nrm3266>.
24. Bonazzi M, Spano S, Turacchio G, Cericola C, Valente C, Colanzi A, Kweon HS, Hsu VW, Polishchuck EV, Polishchuck RS, Sallase M, Pulvirenti T, Corda D, Luini A. 2005. CtBP3/BARS drives membrane fission in dynamin-independent transport pathways. *Nat Cell Biol* 7:570–580. <http://dx.doi.org/10.1038/ncb1260>.
25. Macia E, Ehrlich M, Massol R, Boucrot E, Brunner C, Kirchhausen T. 2006. Dynasore, a cell-permeable inhibitor of dynamin. *Dev Cell* 10:839–850. <http://dx.doi.org/10.1016/j.devcel.2006.04.002>.
26. Ehrlich M, Boll W, Van Oijen A, Hariharan R, Chandran K, Nibert ML, Kirchhausen T. 2004. Endocytosis by random initiation and stabilization of clathrin-coated pits. *Cell* 118:591–605. <http://dx.doi.org/10.1016/j.cell.2004.08.017>.
27. Boucrot E, Saffarian S, Zhang R, Kirchhausen T. 2010. Roles of AP-2 in clathrin-mediated endocytosis. *PLoS One* 5:e10597. <http://dx.doi.org/10.1371/journal.pone.0010597>.
28. Merz A, Long G, Hiet MS, Brugger B, Chlanda P, Andre P, Wieland F, Krijnse-Locker J, Bartenschlager R. 2011. Biochemical and morphological properties of hepatitis C virus particles and determination of their lipidome. *J Biol Chem* 286:3018–3032. <http://dx.doi.org/10.1074/jbc.M110.175018>.
29. Nielsen SU, Bassendine MF, Martin C, Lowther D, Purcell PJ, King BJ, Neely D, Toms GL. 2008. Characterization of hepatitis C RNA-containing particles from human liver by density and size. *J Gen Virol* 89:2507–2517. <http://dx.doi.org/10.1099/vir.0.2008/000083-0>.
30. Klausner RD, Donaldson JG, Lippincott-Schwartz J. 1992. Brefeldin A: insights into the control of membrane traffic and organelle structure. *J Cell Biol* 116:1071–1080. <http://dx.doi.org/10.1083/jcb.116.5.1071>.
31. Deborde S, Perret E, Gravotta D, Deora A, Salvatore S, Schreiner R, Rodriguez-Boulant E. 2008. Clathrin is a key regulator of basolateral polarity. *Nature* 452:719–723. <http://dx.doi.org/10.1038/nature06828>.
32. Gan Y, McGraw TE, Rodriguez-Boulant E. 2002. The epithelial-specific adaptor AP1B mediates post-endocytic recycling to the basolateral membrane. *Nat Cell Biol* 4:605–609. <http://dx.doi.org/10.1038/ncb827>.
33. Gravotta D, Carvajal-Gonzalez JM, Mattera R, Deborde S, Banfelder JR, Bonifacino JS, Rodriguez-Boulant E. 2012. The clathrin adaptor AP-1A mediates basolateral polarity. *Dev Cell* 22:811–823. <http://dx.doi.org/10.1016/j.devcel.2012.02.004>.
34. Bishe B, Syed GH, Field SJ, Siddiqui A. 2012. Role of phosphatidylinositol 4-phosphate (PI4P) and its binding protein GOLPH3 in hepatitis C virus secretion. *J Biol Chem* 287:27637–27647. <http://dx.doi.org/10.1074/jbc.M112.346569>.
35. Lu X, Mehta A, Dadmarz M, Dwek R, Blumberg BS, Block TM. 1997. Aberrant trafficking of hepatitis B virus glycoproteins in cells in which N-glycan processing is inhibited. *Proc Natl Acad Sci U S A* 94:2380–2385. <http://dx.doi.org/10.1073/pnas.94.6.2380>.
36. Tang Y, Leao IC, Coleman EM, Broughton RS, Hildreth JE. 2009. Deficiency of Niemann-Pick type C-1 protein impairs release of human immunodeficiency virus type 1 and results in Gag accumulation in late endosomal/lysosomal compartments. *J Virol* 83:7982–7995. <http://dx.doi.org/10.1128/JVI.00259-09>.
37. Neveu G, Barouch-Bentov R, Ziv-Av A, Gerber D, Jacob Y, Einar S. 2012. Identification and targeting of an interaction between a tyrosine motif within hepatitis C virus core protein and AP2M1 essential for viral assembly. *PLoS Pathog* 8:e1002845. <http://dx.doi.org/10.1371/journal.ppat.1002845>.
38. Wernet-Hammond ME, Lauer SJ, Corsini A, Walker D, Taylor JM, Rall SC, Jr. 1989. Glycosylation of human apolipoprotein E. The carbohydrate attachment site is threonine 194. *J Biol Chem* 264:9094–9101.
39. Rodriguez-Boulant E, Kreitzer G, Musch A. 2005. Organization of vesicular trafficking in epithelia. *Nat Rev Mol Cell Biol* 6:233–247. <http://dx.doi.org/10.1038/nrm1593>.
40. Ivanovic T, Boulant S, Ehrlich M, Demidenko AA, Arnold MM, Kirchhausen T, Nibert ML. 2011. Recruitment of cellular clathrin to viral factories and disruption of clathrin-dependent trafficking. *Traffic* 12:1179–1195. <http://dx.doi.org/10.1111/j.1600-0854.2011.01233.x>.
41. Mee CJ, Farquhar MJ, Harris HJ, Hu K, Ramma W, Ahmed A, Maurel P, Bicknell R, Balfe P, McKeating JA. 2010. Hepatitis C virus infection reduces hepatocellular polarity in a vascular endothelial growth factor-dependent manner. *Gastroenterology* 138:1134–1142. <http://dx.doi.org/10.1053/j.gastro.2009.11.047>.
42. Konan KV, Giddings TH, Jr, Ikeda M, Li K, Lemon SM, Kirkegaard K. 2003. Nonstructural protein precursor NS4A/B from hepatitis C virus alters function and ultrastructure of host secretory apparatus. *J Virol* 77:7843–7855. <http://dx.doi.org/10.1128/JVI.77.14.7843-7855.2003>.